Aging and structural relaxation of hyper-quenched $Mg_{65}Cu_{25}Y_{10}$ metallic glass

Fuqiang Zhai[a], Eloi Pineda[b], Beatrice Ruta[c], Marta Gonzalez-Silveira[d], Daniel Crespo[a]

[a]Dept. Física Aplicada, EPSC, Universitat Politècnica Catalunya - BarcelonaTech, Esteve Terradas 5, 08860 Castelldefels, Spain.
fuqiangzhai@gmail.com / daniel.crespo@upc.edu

[b]Dept. Física i Enginyeria Nuclear, ESAB, Universitat Politècnica Catalunya - BarcelonaTech, Esteve Terradas 8, 08860 Castelldefels, Spain.
eloi.pineda@upc.edu

[c]European Synchrotron Radiation Facility, BP220, F-38043, Grenoble cedex, France.
beatrice.ruta@esrf.fr

[d]Nanomaterials and Microsystems Group, Physics Department, Universitat Autònoma Barcelona, 08193 Bellaterra, Spain.

[*]Corresponding author:
Daniel Crespo
daniel.crespo@upc.edu
Tel. (34) 934 134 141
Fax. (34) 934 137 007

Abstract

The structural relaxation, glass transition and crystallization processes of $Mg_{65}Cu_{25}Y_{10}$ metallic glass are studied by Differential Scanning Calorimetry (DSC) and Mechanical Spectroscopy. The relaxation model derived from the mechanical measurements is compared with the kinetics of these transformations obtained from the DSC curves. The structural relaxation kinetics is found to be controlled by the glassy dynamics following an Adams-Gibbs-Vogel function. The glass transition and crystallization kinetics are controlled by the dynamics of the supercooled melt following a Vogel-Fulcher-Tammann behaviour. The results suggest that the microscopic processes responsible of structural relaxation and aging below the glass transition correspond to the same processes generating the α-relaxation peak.

1. Introduction

Physical properties of metallic glasses (MG) can be deeply affected by the relaxation state attained during the previous thermal history [1]. The high cooling rates usually needed to bypass crystallization result in glasses with high fictive temperatures (T_f). This as-quenched state is characterized by large amounts of excess free volume and internal stresses in the glass structure and it can be stabilized through annealing or physical aging. In Mg, Ca and Ce-based metallic glasses, where the glass transition temperature (T_g) is found below 450 K, the structural relaxation processes are active even at room temperature. A clear understanding and description of the processes driving structural relaxation is then a fundamental knowledge in designing the annealing protocols in order to obtain the desired properties and in predicting the time evolution of the physical properties under working conditions.

In Ref. [2] we described the relaxation spectrum of $Mg_{65}Cu_{25}Y_{10}$ glass by means of mechanical spectroscopy. The elastic complex modulus measured in the multi-frequency tests was well described by considering that the system follows a Vogel-Fulcher-Tammann (VFT) function in the supercooled liquid state

$$\tau_e(T) = \tau_0 \exp\left(\frac{B}{(T - T_0)}\right) \quad (1)$$

and an Adams-Gibbs-Vogel (AGV) function [3] in the out-of-equilibrium glassy state

$$\tau_{ne}(T) = \tau_0 \exp\left(\frac{B}{T\left(1 - T_0/T_f\right)}\right) \quad (2)$$

with parameters B=5750 and T_0=260 K taken from viscosity data [4] and $\tau_0=2.4\times10^{-15}$ s determined from the position of the maximum of the loss peak in the equilibrium supercooled liquid region. The fictive temperature changed from T_{f2}=437 K in the as-quenched state to T_{f1}=412 K in a relaxed state obtained by isothermal annealing. The onset of glass transition was observed by DSC at T_g=416 K when heating at 10 K/min. The relaxation time given by equations 1 and 2 correspond to the main structural relaxation time of the system (α-relaxation). Below T_g, the dynamics of the glass are arrested in an Arrhenius behaviour while, above T_g, the VFT function reproduces the diverging slowing down of the dynamics when approaching glass transition.

The microscopic processes leading to structural relaxation and physical aging of metallic glasses are not at all clear. Mechanical spectroscopy at low frequencies (0-200Hz) shows that the internal friction increases in the same temperature region were structural relaxation of as-

quenched samples takes place [5][6]. In many systems it is considered that the structural relaxation is driven by secondary relaxations faster than the main relaxation of the glass [7] [8] [9]. Evident secondary relaxations have been found in Pd-based and La-based systems [6]. In other systems, the increase of internal friction is observed as a low temperature excess wing of the equilibrium α-relaxation peak in the viscoelastic loss modulus [10] [11] [12]. In reference [2] the excess wing of $Mg_{65}Cu_{25}Y_{10}$ glass was well described as the high frequency tail of the α-relaxation once arrested in the non-equlibrium dynamics given by equation 2.

If the microscopic processes driving structural changes during annealing or aging of metallic glasses are the same processes generating internal friction in mechanical spectroscopy experiments, the determination of the relaxation model would be a useful tool for understanding such phenomena. In this paper we will compare results of Differential Scanning Calorimetry (DSC) and Dynamo-Mechanical Analysis (DMA) of $Mg_{65}Cu_{25}Y_{10}$. The measurements were performed in samples with different relaxation states obtained by annealing or by room-temperature aging. The aim of the work is to check if the structural changes occurring during annealing and aging of as-quenched samples are explained by the relaxation model proposed in reference [2] and, therefore, if they can be fundamentally described by equations 1 and 2.

2. Materials and methods

Samples were produced as thin ribbons by melt-spinning. Cu and Y pure metals were pre-alloyed by arc-melting under Ti-gettered Ar atmosphere. Pure Mg was added in an induction furnace in order to prevent its volatilization. The melt was then injected on the Cu wheel spinning at 40 m/s perimeter velocity producing rapidly quenched metallic ribbons with thickness of 33±4 μm. Differential scanning calorimetry (DSC) was performed on a NETZSCH DSC 404 F3 Pegasus and in a Perkin Elmer DSC-7. In order to assess the kinetics of the reactions the DSC curves were performed with heating rates from 5 to 60 K/min on the as-quenched sample and from 0.5 to 60 K/min on the aged samples. Mechanical spectroscopy was performed on a TA-instruments Q800 DMA. Tests were carried on in tensile geometry applying a preload (static force) of 0.08 N at a frequency of 1 Hz. Oscillating strains of 1 μm amplitude were applied by loading and unloading around this static value with the required dynamic force. The length of the ribbon pieces was of 10mm.

The measurements were performed on as-quenched, relaxed and aged samples. The as-quenched samples were stored several weeks at room temperature before the measurements, the fast physical aging observed during the first days after the production of rapidly-quenched $Mg_{65}Cu_{25}Y_{10}$ glass [13] is then expected not to affect the results. The relaxed samples measured

by DMA were obtained by annealing isothermally during 30 min at 410 K while being under tensile constant load of 0.08 N. This procedure is expected to release most part of quenched-in internal stresses and suppress sensible structural changes when annealing with the heating rates used in the DSC and DMA experiments (0.5 – 60 K/min). The aged samples were obtained by keeping the ribbons in a humidity-free environment during 20 and 24 months.

3. Results

Figure 1 shows the signature of structural relaxation of as-quenched samples measured by DSC and DMA. The blue lines correspond to the as-quenched samples. Above 365 K, the increase of the loss modulus measured at 1 Hz corresponds well with the onset of the exothermic signal of the structural relaxation. Between 365 K and 400 K the loss modulus $E''(\omega,T)$ shows an evident hump in the same region where the structural relaxation is detected by the DSC signal. Here it should be noted that the change of frequency in DMA experiments, and the change of heating rate in both DSC and DMA would shift the temperatures were the different phenomena are observed. However, from the comparison of DSC and DMA measurements, it seems plausible that the same microscopic events generating internal friction are also responsible of the structural changes stabilizing the system.

For the 5 K/min DSC scan depicted in the figure, the glass transition region is detected between 408 K and 428 K. Above this temperature the system reaches internal equilibrium. The maximum of the loss modulus peak, which would mark the dynamic glass transition corresponding to a frequency of 1 Hz, is observed near 440 K well above the glass transition detected by DSC, which would correspond to the dynamic glass transition at frequencies approximately 100 times lower [14].

For the relaxed samples (red lines) the release of heat during annealing is completely absent in the DSC signal, this means that the system remains basically in the same isoconfigurational state below T_g. In the loss modulus, the low temperature hump is suppressed but the increase of internal friction is still observed as a low-temperature wing of the equilibrium. This means the microscopic processes generating internal friction are also activated in the relaxed state but, in this case, they do not lead the system to a change of state.

Figure 2 shows the change in the intensity and onset of structural relaxation between as-quenched samples and samples stored 20 months. It can be observed that, after the fast physical aging observed during the first weeks after production [13], $Mg_{65}Cu_{25}Y_{10}$ is continuously evolving towards more and more stable states due to aging at room temperature. Figure 2 inset shows the change in the onset temperatures of structural relaxation and glass transition when

applying different heating rates. In this case the measurements correspond to samples stored 24 months.

The activation energies of the structural relaxation, glass transition and crystallization processes have been calculated by the Kissinger method, the calculated values are E_r=148 kJ/mol, E_g=303 kJ/mol and E_x=208 kJ/mol respectively. Figure 3 shows the Kissinger plots of as-quenched, 20-months and 24-months samples. The temperatures used to obtain the Kissinger plots correspond to the maximum of heat release detected by DSC for the structural relaxation and crystallization processes and to the inflection point in the specific heat curve during the glass transition. As expected, the crystallization temperatures depend on the kinetics of the metastable equilibrium melt and hence they are not affected by the aging of the samples.

4. Discussion

The loss modulus peak measured in constant heating rate DMA tests is composed of a non-equilibrium ($T<T_{g,R}$) and an equilibrium region ($T>T_{g,R}$), where $T_{g,R}$ is the glass transition temperature at the corresponding heating rate R. In tensile DMA experiments, the frequency response to the mechanical perturbations is described by a complex Young modulus $E^*(\omega,T)=E'(\omega,T)+iE''(\omega,T)$. In ref. [2] the frequency response of $Mg_{65}Cu_{25}Y_{10}$ was found well described by a Cole-Cole (CC) relaxation function

$$E^*(\omega,T) = E_0(T)\left[1-\frac{1}{1+\left(i\omega\tau(T)\right)^{\alpha}}\right] \qquad (3)$$

with broadening parameter α=0.4-0.5 for both the supercooled liquid (equilibrium region) and the relaxed glass, and α=0.7 for the as-quenched glass. The empirical CC-function is commonly used to rationalize the frequency response of glasses [15]. In the case of $Mg_{65}Cu_{25}Y_{10}$ this function was able to describe the high-frequency (or equivalently the low-temperature) side of the loss peak, which is the side accessible in the tensile experiments used in this work.

Figure 1 (thin solid lines) shows the theoretical $E''(\omega_0,T)$ functions obtained from equation 3 substituting $\omega_0=2\pi$ s^{-1} and $\tau(T)=\tau_{ne}(T)$ (equation 2). The fictive temperatures and broadening parameters are α_1=0.5, T_{f1}=412 K and α_2=0.7, T_{f2}=437 K for the relaxed and as-quenched states respectively. For the relaxed samples, the combination of equations 2 and 3 follows the experimental $E''(\omega_0,T)$ behaviour until the system enters the glass transition region above $T_{g,1K/min}$=401 K. The loss modulus of the relaxed glass is then well described by a unique fictive temperature T_{f1} very close to the temperature of the isothermal relaxation treatment. In the equilibrium region above the glass transition, $E''(\omega_0,T)$ corresponds to a CC-relaxation function

with τ(T) following a VFT behaviour (combination of equations 1 and 3) with the maximum of the loss peak at the temperature were $\tau_e(T)=1/\omega_0$.

For the as-quenched samples, the combination of equations 2 and 3 only describes the response of the system during a short region between 360 K and 370 K. Above this region, the irreversible structural relaxation drives the system through different glassy states and a constant fictive temperature is not able to describe the $E''(\omega_0,T)$ behaviour anymore. The change in the broadening exponent α between as-quenched and relaxed states may be an artifact due to the short fitting region available in the as-quenched samples. However, a change in the exponent of the correlation functions for different relaxation states was also observed by X-ray Photon Correlation Spectroscopy in the same material [16].

The activation energies for the different processes are obtained from the T^2/R vs $1/T$ curves shown in figure 3 as

$$\frac{E}{k_B T} = \ln\left(\frac{T^2}{R}\right) + \ln(A) \tag{4}$$

where A is a constant value. The use of the transformation curves T^2/R vs $1/T$ for calculating activation energies is based on considering that the activation energy is constant over temperature and time. Although this is not fulfilled in the case of the reactions studied here, it is a robust method for estimating average activation energies. The coincidence between the activation energies of viscous flow and the ones calculated from the rate of thermal measurements by equation 3 is a well-known fact and it is used in metallic glasses since the work of Chen [17].

Now we will compare the kinetics measured by DSC with the relaxation scheme proposed by equations 1, 2 and 3 and the parameters B and T_0 reported above. The glass transition and crystallization kinetics are controlled by the melt viscosity. The local activation energies are then given by the VFT function and can be calculated as $E/k_B=BT^2/(T-T_0)^2$. Substituting the temperatures corresponding to the inflection point of the glass transition, $T_{gi,20K/min}$=430 K, and the maximum of the crystallization peak, $T_{x,20K/min}$=480 K, the local activation energies are $E_{g,VFT}$=305 kJ/mol and $E_{x,VFT}$=227 kJ/mol. These are in agreement with the average activation energies E_g=303 kJ/mol and E_x=208 kJ/mol obtained by the Kissinger method and reported above. The kinetics of the structural relaxation is controlled by the non-equilibrium relaxation times given by equation 2, the activation energy can be calculated as $E/k_B=B/(1-T_0/T_f)$. The activation energies for the relaxed (T_{f1}) and as-quenched (T_{f2}) states go from $E_{r,Tf1}$=129 kJ/mol to

$E_{r,Tf2}$=118 kJ/mol. This is also close to the activation energy E_r=148 kJ/mol calculated from the DSC temperatures.

Following ref. [17], in figure 4 we depict a visual image of the degree of agreement between the activation energies calculated from the Kissinger plots and the relaxation times given by equations 1 and 2. With a proper time constant shift *A*, the transformation curves T^2/R vs $1/T$ are compared with the equilibrium and non-equilibrium relaxation times $\tau(T)$. Figure 4 shows all the measurements performed in as-quenched and aged samples. The different degree of aging results in the scatter of the data corresponding to the structural relaxation temperature while it has not significant effect on the glass transition and crystallization temperatures.

Another common way of determining the kinetics of glasses and melts from the characteristic temperatures measured by DSC is considering that the inverse of the heating rate $1/R$ is proportional to the characteristic time of the detected process [18] [19]. For instance, the relation between $1/R$ and the onset of glass transition detected by DSC is commonly used to estimate the fragility parameter of glass-forming metallic liquids [20]. Figure 5 shows the $1/R$ vs T curves corresponding to the onset of structural relaxation and the inflection point of the glass transition, in this case without any shifting parameter. Diamonds correspond to the experimental values of τ(T) obtained for the relaxed samples by multi-frequency DMA tests [2]. The solid lines correspond again to the $\tau(T)$ functions given by equations 1 and 2.

The $1/R$ vs T curves for the onset of structural relaxation correspond well with the non-equilibrium dynamics given by equation 2, the shift due to the aging can be explained as a decrease in the fictive temperature reaching T_{f3}~422 K for the samples aged 24 months. The curve corresponding to the inflection point of the glass transition is parallel to the equilibrium dynamics given by equation 1. The dashed lines mark the limits of the dynamic glass transition region estimated by equation 3, the $1/R$ vs T curves for the onset and end of glass transition temperatures measured in the DSC scans (not shown in the figure) correspond well with this limits. Finally, the extrapolation of the map to lower temperatures shows that the relaxation times at room temperature are τ=9 days for the as-quenched samples, and τ=130 days for the aged samples.

5. Conclusions

The analysis of mechanical spectroscopy data suggest the relaxation of $Mg_{65}Cu_{25}Y_{10}$ glass can be understood by a single α-relaxation process following VFT behaviour in the metastable equilibrium region and an Arrhenius behaviour below T_g. The comparison of equations 1, 2 and

3 with DMA and DSC data shows that the kinetics of structural relaxation, glass transition and crystallization of $Mg_{65}Cu_{25}Y_{10}$ can be understood by the proposed relaxation model.

Acknowledgements

We thank Dr. Pere Bruna for fruitful and valuable discussions. Work funded by CICYT grant MAT2010-14907 and Generalitat de Catalunya grant 2009SGR1251. Fuqiang Zhai thanks China Scholarship Council (CSC) for providing his scholarship.

References

[1] G. Kumar, P. Neibecker, Y.H. Liu, J. Schroers, Critical fictive temperature for plasticity in metallic glasses, Nature Communications 4 (2013) 1536.

[2] E. Pineda, P. Bruna, B. Ruta, M. Gonzalez-Silveira, D. Crespo, Relaxation of rapidly quenched metallic glasses: Effect of relaxation state on the slow low temperature dynamics, Acta Mater. 61 (2013) 3002.

[3] I. HODGE, Effects of Annealing and Prior History on Enthalpy Relaxation in Glassy-Polymers .6. Adam-Gibbs Formulation of Nonlinearity, Macromolecules 20 (1987) 2897-2908.

[4] R. Busch, W. Liu, W. Johnson, Thermodynamics and kinetics of the Mg65Cu25Y10 bulk metallic glass forming liquid, J.Appl.Phys. 83 (1998) 4134-4141.

[5] J.C. Qiao, J.M. Pelletier, Kinetics of structural relaxation in bulk metallic glasses by mechanical spectroscopy: Determination of the stretching parameter beta(KWW), Intermetallics 28 (2012) 40-44.

[6] J.C. Qiao, J.M. Pelletier, Dynamic mechanical analysis in La-based bulk metallic glasses: Secondary (beta) and main (alpha) relaxations, J.Appl.Phys. 112 (2012) 083528.

[7] J. Hachenberg, D. Bedorf, K. Samwer, R. Richert, A. Kahl, M.D. Demetriou et al., Merging of the alpha and beta relaxations and aging via the Johari-Goldstein modes in rapidly quenched metallic glasses, Appl.Phys.Lett. 92 (2008) 131911.

[8] L. Hu, Y. Yue, Secondary Relaxation in Metallic Glass Formers: Its Correlation with the Genuine Johari-Goldstein Relaxation RID H-1313-2011, J.Phys.Chem.C 113 (2009) 15001-15006.

[9] Z. Wang, H.B. Yu, P. Wen, H.Y. Bai, W.H. Wang, Pronounced slow beta-relaxation in La-based bulk metallic glasses RID E-5312-2010, J.Phys.-Condes.Matter 23 (2011) 142202.

[10] K. Ngai, Johari-Goldstein relaxation as the origin of the excess wing observed in metallic glasses, J.Non Cryst.Solids 352 (2006) 404-408.

[11] J. Hachenberg, K. Samwer, Indications for a slow beta-relaxation in a fragile metallic glass, J.Non Cryst.Solids 352 (2006) 5110-5113.

[12] J.C. Qiao, J.M. Pelletier, Mechanical relaxation in a Zr-based bulk metallic glass: Analysis based on physical models, J.Appl.Phys. 112 (2012) 033518.

[13] A. Castellero, B. Moser, D.I. Uhlenhaut, F.H. Dalla Torre, J.F. Loeffler, Room-temperature creep and structural relaxation of Mg-Cu-Y metallic glasses, Acta Mater. 56 (2008) 3777-3785.

[14] O.V. Mazurin, Problems of compatibility of the values of glass transition temperatures published in the world literature, Glass Phys.Chem. 33 (2007) 22-36.

[15] C. Svanberg, Correlation function for relaxations in disordered materials, J.Appl.Phys. 94 (2003) 4191-4197.

[16] B. Ruta, Y. Chushkin, G. Monaco, L. Cipelletti, E. Pineda, P. Bruna et al., Atomic-Scale Relaxation Dynamics and Aging in a Metallic Glass Probed by X-Ray Photon Correlation Spectroscopy, Phys.Rev.Lett. 109 (2012) 165701.

[17] H. CHEN, Method for Evaluating Viscosities of Metallic Glasses from Rates of Thermal Transformations, J.Non Cryst.Solids 27 (1978) 257-263.

[18] D. Perera, Compilation of the fragility parameters for several glass-forming metallic alloys, J.Phys.-Condes.Matter 11 (1999) 3807-3812.

[19] D. Perera, A. Tsai, Thermal and viscoelastic properties of a strong bulk metallic glass former, J.Phys.D-Appl.Phys. 33 (2000) 1937-1946.

[20] W.H. Wang, Correlations between elastic moduli and properties in bulk metallic glasses, J.Appl.Phys. 99 (2006) 093506.

Figure captions

Figure 1. DSC and DMA runs obtained for the as-quenched (blue) and relaxed (red) samples. Thin lines correspond to the $E''(T)/E_0$ calculated from the CC-function and the proposed non-equilibrium dynamics $\tau_{ne}(T,T_f)$.

Figure 2. DSC curves obtained for as-quenched (blue), 20-months aged (purple) and 24-months aged (magenta). The inset shows the temperature shift of structural relaxation and glass transition as function of the applied heating rate.

Figure 3. Kissinger plots for the temperatures of the crystallization peak (downwards triangles), glass transition inflection point (circles) and structural relaxation maximum (upwards triangles). The temperatures are obtained from DSC curves of as-quenched (blue symbols), 20-months aged (purple symbols) and 24-months aged (magenta symbols) samples.

Figure 4. T^2R^{-1} vs $1/T$ curves for crystallization peak (downwards triangles), glass transition inflection point (circles) and structural relaxation maximum (upwards triangles). In the case of structural relaxation the colours correspond to as-quenched (blue symbols), 20-months aged (purple symbols) and 24-months aged (magenta symbols) samples. Solid lines correspond to the equilibrium and non-equilibrium dynamics given by equations 1 and 2. The T^2R^{-1} vs $1/T$ curves are shifted by appropriate values of the A constant for each one of the three processes.

Figure 5. Relaxation times of the relaxed samples obtained by DMA (diamonds). $1/R$ vs T curves for the glass transition inflection point (circles) and the onset of structural relaxation (upwards triangles). In the case of structural relaxation the colours correspond to as-quenched (blue symbols), 20-months aged (purple symbols) and 24-months aged (magenta symbols) samples. Solid lines correspond to the equilibrium and non-equilibrium dynamics given by equations 1 and 2.

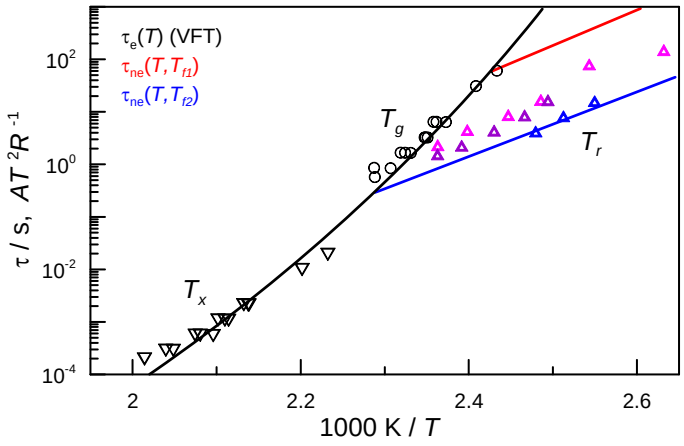
τe(T) (VFT)
τne(T,Tf1)
τne(T,Tf2)
Tg
Tr
Tx
τ / s, AT 2R -1
1000 K / T
10^2
10^0
10^-2
10^-4
2
2.2
2.4
2.6

Figure 4

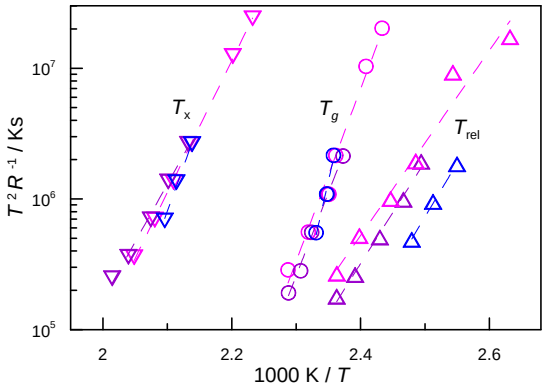

Figure 3

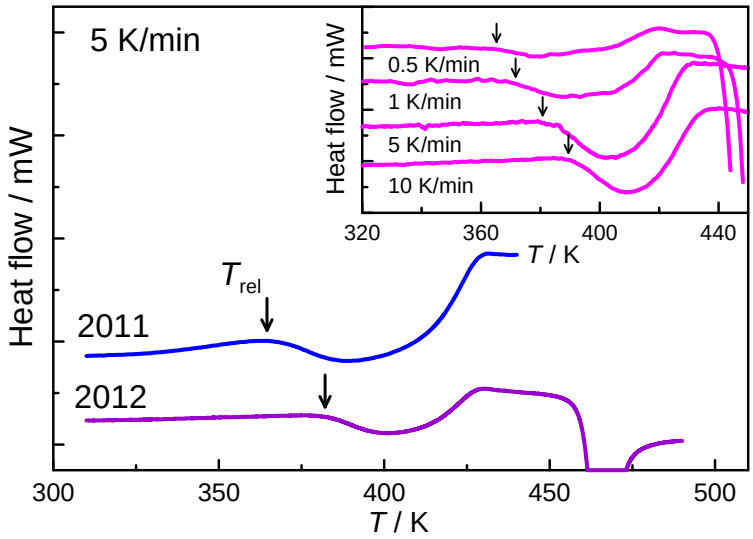
5 K/min
Heat flow / mW
0.5 K/min
1 K/min
5 K/min
10 K/min
320
360
400
440
T / K
T rel
2011
2012
300
350
400
450
500
T / K

Figure 2

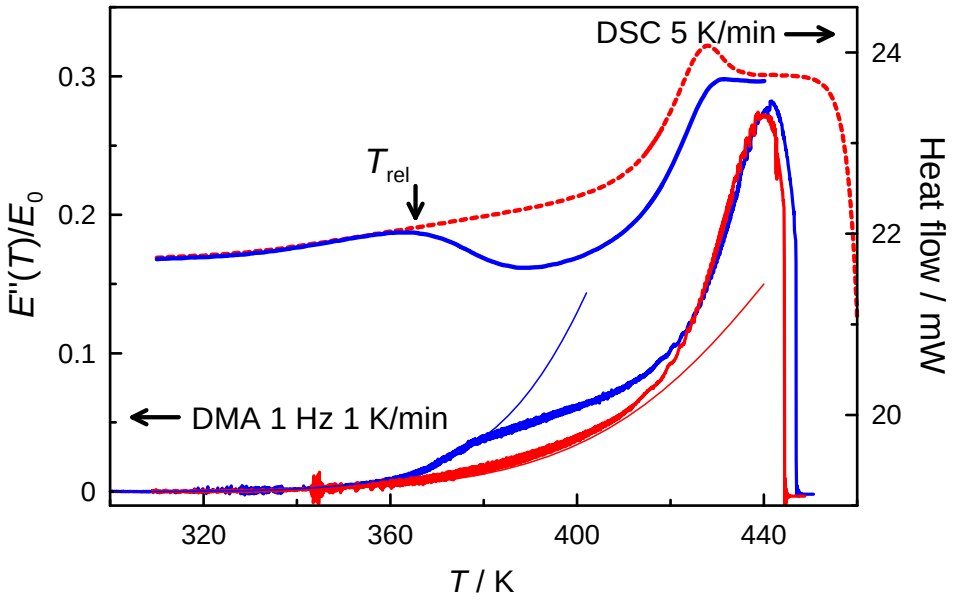
DSC 5 K/min
T_{rel}
DMA 1 Hz 1 K/min
$E'(T)/E_0$
Heat flow / mW
T / K
0
0.1
0.2
0.3
20
22
24
320
360
400
440

Figure 1

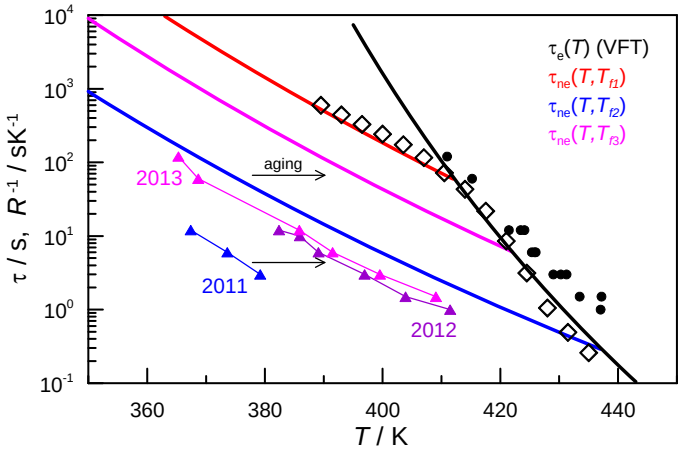
τ / s, R-1 / sK-1
T / K
τe(T) (VFT)
τne(T,Tf1)
τne(T,Tf2)
τne(T,Tf3)
aging
2013
2011
2012

Figure 5